Inorg. Chem. **2008**, *47*, 11535−11542

Tossing and Turning: Guests in the Flexible Frameworks of Metal(III) Dicarboxylates

Marie Vougo-Zanda, Jin Huang, Ekaterina Anokhina,† Xiqu Wang, and Allan J. Jacobson*

Department of Chemistry, University of Houston, Houston, Texas 77204-5003

Received January 2, 2008

Single crystals of $Ga(OH)(C_8H_4O_4)\cdot 0.74C_8H_6O_4$ (**2**) and $Ga(OH,F)(C_8H_4O_4)\cdot 0.74C_8H_6O_4$ (**3**) were obtained under hydrothermal conditions. The structures of **2** and **3** have the same topological framework as the previously reported aluminum 1,4-benzenedicarboxylate (BDC), $Al(OH)(C_8H_4O_4)\cdot 0.7C_8H_6O_4$ (**1**). The frameworks are built by interconnecting M−OH−M chains (M = Al, Ga) with BDC anions to form large diamond-shaped one-dimensional channels filled with additional H_2BDC guest molecules occupying disordered positions in the channels. Upon removal of H_2BDC, other guest molecules such as H_2O and pyridine can be inserted. In this work, we present a study of the intercalation of aromatic guests (BDC and pyridine) into frameworks of **1**−**3** by liquid and vapor diffusion into the empty channels of **1** and by single-crystal-to-single-crystal solvothermal guest exchange for **2** and **3**. In the case of Al(OH)BDC and Ga(OH,F)BDC, two interconvertible, guest-concentration-dependent phases with different orientations of the pyridine guests have been observed, while only one pyridine orientation is found in Ga(OH)BDC.

Introduction

Intensive studies in the area of coordination polymers recently led to the discovery of so-called third-generation materials, i.e., solids with flexible, "dynamic" frameworks that respond to changes in, for example, the guest concentration or external pressure and which have the potential to be used as sensors in addition to conventional applications for microporous materials such as gas sorption, separation, and catalysis.[1–7] One of the most remarkable examples of the flexible coordination frameworks is the series $M^{III}(OH)BDC\cdot x H_2BDC$ (BDC = 1,4-benzendicarboxylate; M = V,[8,9] Cr,[10,11] Al,[12] In[13]) where the chains of trans corner-sharing MO_6 octahedra are bridged by BDC ligands to generate three-dimensional frameworks with rhombic channels. As synthesized, the compounds contain hydrogen-bonded chains of the guest H_2BDC molecules[13] inside the channels that can be removed by heating, leading to porous frameworks (except for In) of high thermal stability (up to 500 °C). Once the channels are empty, other species may be reversibly intercalated. Upon the intercalation, the channels contract in an accordion-like manner, so that the cell dimensions perpendicular to the chains change to accommodate the specific guest molecules and remain virtually constant in the direction of the chains regardless of the guest species. This phenomenon was referred to as the "breathing effect" and was studied in detail on polycrystalline samples for the case of hydration of the aluminum derivative.[12]

* To whom correspondence should be addressed. E-mail: ajjacob@uh.edu. Telephone: (713) 743-2785. Fax: (713) 743-2787.
† Deceased.

(1) Kitagawa, S.; Kitaura, R.; Noro, S. *Angew. Chem., Int. Ed.* **2004**, *43*, 2334.
(2) Kaneko, W.; Ohba, M.; Kitagawa, S. *J. Am. Chem. Soc.* **2007**, *129*, 13706.
(3) Yanai, N.; Kaneko, W.; Yoneda, K.; Ohba, M.; Kitagawa, S. *J. Am. Chem. Soc.* **2007**, *129*, 3496.
(4) Rosseinsky, M. J. *Microporous Mesoporous Mater.* **2004**, *73*, 15.
(5) Hawxwell, S. M.; Espallargas, G. M.; Bradshaw, D.; Rosseinsky, M. J.; Prior, T. J.; Florence, A. J.; van de Streek, J.; Brammer, L. *Chem. Commun.* **2007**, 1532.
(6) Fletcher, A. J.; Thomas, K. M.; Rosseinsky, M. J. *J. Solid State Chem.* **2005**, *178*, 2491.
(7) Serre, C.; Mellot-Draznieks, C.; Surble, S.; Audebrand, N.; Filinchuk, Y.; Férey, G. *Science* **2007**, *315* (5820), 1828.
(8) Barthelet, K.; Marrot, J.; Riou, D.; Férey, G. *Angew. Chem., Int. Ed.* **2002**, *41*, 281.
(9) Barthelet, K.; Marrot, J.; Férey, G.; Riou, D. *Chem. Commun.* **2004**, 520.
(10) Serre, C.; Millange, F.; Thouvenot, C.; Nogues, M.; Marsolier, G.; Louer, D.; Férey, G. *J. Am. Chem. Soc.* **2002**, *124*, 13519–13526.
(11) Férey, G.; Latroche, M.; Serre, C.; Millange, F.; Loiseau, T.; Percheron-Guega, A. *Chem. Commun.* **2003**, 2976.
(12) Loiseau, T.; Serre, C.; Huguenard, C.; Fink, G.; Taulelle, F.; Henry, M.; Bataille, T.; Férey, G. *Chem.—Eur. J.* **2004**, *10*, 1373.
(13) Anokhina, E. V.; Vougo-Zanda, M.; Wang, X.; Jacobson, A. J. *J. Am. Chem. Soc.* **2005**, *127*, 15000.

10.1021/ic800008f CCC: $40.75
Published on Web 04/23/2008

Table 1. Crystallographic Data for Compounds **1**−**3**

	1	**2**	**3**
chemical formula	$Al(OH)(C_8H_4O_4)\cdot 0.7C_8H_6O_4$	$Ga(OH)(C_8H_4O_4)\cdot 0.74C_8H_6O_4$	$Ga(OH,F)(C_8H_4O_4)\cdot 0.74C_8H_6O_4$
fw	324.29	373.79	373.94
cryst syst	orthorhombic	orthorhombic	orthorhombic
space group	*Pnma*	*Pnma*	*Pnma*
a, Å	17.019(4)	17.525(4)	17.410(3)
b, Å	6.584(2)	6.7216(16)	6.7444(10)
c, Å	12.262(3)	11.893(3)	12.1646(17)
V, Å^3	1374.1(6)	1401.0(6)	1428.4(4)
Z	4	4	4
temp, K	293	293	293
μ(Mo Kα), mm^{-1}	0.188	2.006	1.967
R1, wR2 [$I > 2\sigma(I)$][a]	0.0503, 0.1385	0.0508, 0.1663	0.0321, 0.1053
R1, wR2 (all data)[a]	0.0700, 0.1524	0.0547, 0.1686	0.0379, 0.1094

[a] $R1 = \sum||F_o| - |F_c||/\sum|F_o|$. $wR2 = [\sum w(F_o^2 - F_c^2)_2/\sum w(F_o^2)^2]^{1/2}$.

Table 2. Crystallographic Data for Compounds **2a**, **3a** and **3b**

	2a	**3a**	**3b**
chemical formula	$Ga(OH)(C_8H_4O_4)\cdot 0.85C_5H_5N$	$Ga(OH,F)(C_8H_4O_4)\cdot C_5H_5N$	$Ga(OH,F)(C_8H_4O_4)\cdot 0.85C_5H_5N$
fw	318.00	330.25	318.40
cryst syst	monoclinic	orthorhombic	orthorhombic
space group	*C*2/*c*	*Imma*	*Imma*
a, Å	19.1213(16)	17.287(11)	18.23(2)
b, Å	11.0629(9)	6.727(5)	6.734(8)
c, Å	6.7261(6)	12.461(9)	11.062(12)
β, deg	108.5120(10)		
V, Å^3	1349.2(2)	1449.2(17)	1358(3)
Z	4	4	4
temp, K	293	293	293
μ(Mo Kα), mm^{-1}	2.014	1.915	2.039
R1, wR2 [$I > 2\sigma(I)$][a]	0.0232, 0.0541	0.0623, 0.1795	0.0737, 0.1755
R1, wR2 (all data)[a]	0.0361, 0.0576	0.0675, 0.1864	0.0838, 0.1815

[a] $R1 = \sum||F_o| - |F_c||/\sum|F_o|$. $wR2 = [\sum w(F_o^2 - F_c^2)_2/\sum w(F_o^2)^2]^{1/2}$.

We have extended this class of compounds to other guest molecules including thiophene, aniline, and acetone in VOBDC[14] and pyridine in Fe(OH)BDC.[15] A single-crystal structure of the latter showed the pyridine molecules to be oriented perpendicular to the iron oxide chains and hydrogen-bonded to the OH group in the Fe−OH−Fe chain. We have extended this work to the synthesis and single-crystal structure determinations of Al(OH)(BDC)·0.7BDC (**1**), Ga(OH)(BDC)·0.74BDC (**2**), and Ga(OH,F)(BDC)·0.74BDC (**3**) frameworks. We present a study of the intercalation of pyridine by liquid and vapor diffusion into the empty channels in these frameworks. In the case of the aluminum host, two interconvertible, guest-concentration-dependent phases, $Al(OH)(C_8H_4O_4)\cdot C_5H_5N$ (**1a**) and $Al(OH)(C_8H_4O_4)\cdot 0.8C_5H_5N$ (**1b**), with different orientations of the pyridine guest molecules have been observed. Two similar phases, $Ga(OH,F)(C_8H_4O_4)\cdot C_5H_5N$ (**3a**) and $Ga(OH,F)(C_8H_4O_4)\cdot 0.85C_5H_5N$ (**3b**), are formed with the gallium host containing fluorine, but only one orientation of pyridine is observed in $Ga(OH)(C_8H_4O_4)\cdot 0.85C_5H_5N$ (**2a**) when fluorine is absent.

Experimental Section

Materials and Methods. All of the reactants were reagent grade and were used as purchased without further purification. The IR spectra were measured on a Galaxy Series FTIR 5000 spectrometer with pressed KBr pellets. Thermogravimetric analysis (TGA) measurements were carried out using a TA Instruments Hi-Res 2950 system in dry air, employing a heating rate of 3 °C min^{-1}. Elemental analyses were performed by Galbraith Laboratories (Knoxville, TN). The powder X-ray diffraction (XRD) patterns were collected at room temperature on a Scintag XDS 2000 (Bragg−Brentano geometry, $\theta-\theta$ mode) laboratory diffractometer with λ(Cu Kα_1, Kα_2) = 1.540 562, 1.544 390 Å. Single-crystal X-ray analyses for **1**−**3** were performed on a Siemens SMART platform diffractometer outfitted with an Apex II area detector and monochromatized graphite Mo Kα radiation. The structures of compounds **1**, **2**, **2a**, **3**, **3a**, and **3b** were solved by direct methods and refined using *SHELXTL*.[16] The structures of **1a** and **1b** were determined from powder XRD data and Rietveld analysis and are discussed in more detail below. Crystal data for the compounds **1**−**3** are summarized in Table 1, and those for compounds **2a**, **3a**, and **3b** are summarized in Table 2.

Host Lattices. Single-Crystal Growth and Characterization of Al(OH)BDC·0.7H$_2$BDC (1). Compound **1** in single-crystal form was synthesized from a mixture of aluminum nitrate nonahydrate (1 mmol), 1,4-benzenedicarboxylic acid (2 mmol), HF (48%, Merck, 0.06 mL), and deionized water (10 mL) in a molar ratio of 1:2:1.5:560. Except for water, the starting components were mixed in a flexible Teflon bag in air. The bag was then put into a hydrothermal reaction vessel containing 10 mL of water and heated at 220 °C for 3 days. After cooling to room temperature, the resulting products were isolated by vacuum filtration, washed with dimethyl sulfoxide (DMSO), followed by deionized H_2O, and then dried in air. DMSO was used to dissolve unreacted H_2BDC. Colorless polyhedra of **1** together with a small amount of an unidentified phase (colorless hexagonal plates) were found in the

(14) Wang, X.; Liu, L.; Jacobson, A. J. *Angew. Chem., Int. Ed.* **2006**, *45*, 6499–6503.
(15) Whitfield, T. R.; Wang, X.; Liu, L.; Jacobson, A. J. *Solid State Sci.* **2005**, *7*, 1096–1103.
(16) Sheldrick, G. M. *SHELXTL, Program for Refinement of Crystal Structures*; Siemens Analytical X-ray Instruments: Madison, WI, 1994.

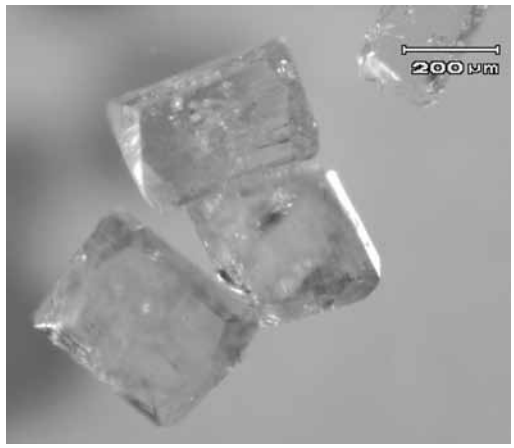

Figure 1. Optical micrograph of crystals of **1**.

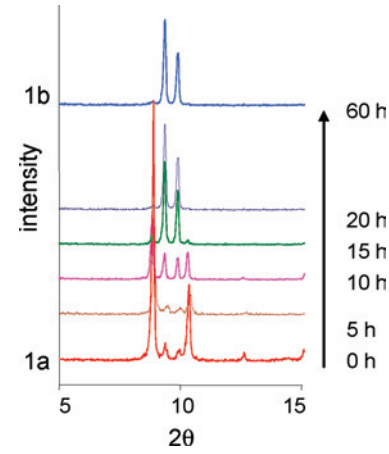

Figure 2. XRD patterns showing the transformation of **1a** to **1b** upon exposure to air.

final products. The final pH was approximately 1−2. Energy-dispersive X-ray analysis showed the absence of fluorine in the crystals of **1**. Optical microscope images of typical polyhedral crystals of **1** are shown in Figure 1.

Systematic synthesis experiments were carried out to optimize the synthesis of **1**. Without the addition of HF, a pure phase of **1** could only be obtained in polycrystalline form or as tiny needles. The presence of HF promoted the appearance of large polyhedral single crystals (up to 0.5 mm in largest dimension) but introduced an additional unidentified phase (colorless hexagonal plates). An excess of HF resulted in the formation of AlF_3 as the final product. Several other synthetic variations and processes including the adjustment of the pH and aluminum sources were attempted, but the synthesis of a pure phase of **1** in single-crystal form was unsuccessful.

Elem anal. for **1**: Al, 8.01% obsd (8.30% calcd); C, 49.19% obsd (50.26% calcd); H, 3.34% obsd (2.83% calcd). The measured chemical composition of **1** is in good agreement with the title formula derived from the structure refinement.

The IR spectrum of **1** (Figure S.1a in the Supporting Information) shows a characteristic stretching frequency of the bridging OH group at 3679 cm^{-1} and a strong band at 1700 cm^{-1} characteristic of a free −C═O vibration, which confirms the presence of free H_2BDC molecules inside the channels.

TGA of **1** shows the release of the BDC molecules in two clearly separated steps. The weight loss from 275 to 400 °C corresponds to the removal of 0.7 mol of H_2BDC molecules (36.00% obsd and 35.84% calcd) from the channels. The second weight loss between 500 and 600 °C corresponds to the loss of 1 mol of coordinated BDC (49.25% obsd and 50.50% calcd) molecules of the framework. These data are consistent with previous reports.[12]

Single-Crystal Growth and Characterization of Ga(OH)BDC·0.74H_2BDC (2) and Ga(OH,F)BDC·0.74H_2BDC (3). Compound **2**, unlike **1**, was obtained in single-crystal form in the absence of fluorine. Compound **2** was synthesized from a mixture of gallium nitrate (1 mmol), 1,4-benzenedicarboxylic acid (2 mmol), and deionized water (10 mL) in a molar ratio of 1:2:560. The starting chemicals were mixed in a flexible Teflon bag in air. The bag was then put into a hydrothermal reaction vessel containing 10 mL of deionized water and heated at 220 °C for 3 days. After quenching to room temperature, the product was filtered, washed with dimethylformamide to dissolve unreacted H_2BDC followed by deionized water, and then dried at room temperature. The final product was a single-phase-containing colorless polyhedra of **2** suitable for single-crystal X-ray measurements. The addition of 1.5 mmol of HF to the above synthetic mixture used for compound **2** results in the formation of colorless single crystals of **3**, a closely related phase where fluorine is incorporated into the compound as shown by elemental analysis. The observed and calculated chemical compositions are as follows. Ga(OH)BDC·0.74H_2BDC (**2**): Ga, 19.30% obsd (18.65% calcd); C, 44.71% obsd (44.69% calcd); H, 2.84% obsd (2.52% calcd). Ga(OH,F)BDC·0.74H_2BDC: (**3**), Ga, 19.10% obsd (18.63% calcd); C, 43.87% obsd (44.67% calcd); H, 2.41% obsd (2.47% calcd); F, 1.20% obsd (1.02% calcd assuming 0.2 F per Ga).

The IR spectra of **2** and **3** also show the characteristic stretching frequency of the bridging OH group observed at 3649 and 3648 cm^{-1} and the strong band at ∼1700 cm^{-1} characteristic of a free −C═O vibration, confirming the presence of the free H_2BDC molecules inside the channels (Figures S.1b and S.1c in the Supporting Information).

TGA data for **2** and **3** were collected in air at 1 °C min^{-1}. Powder XRD experiments show that the final residues were amorphous in each case. Because compound **2** is made up of gallium oxide chains, it is assumed that the final residue is $GaO_{1.5}$. The TGA data show the release of the BDC molecules in two steps. The weight loss from 300 to ∼450 °C corresponds to the removal of 0.74 mol of H_2BDC molecules (31.46% obsd and 32.89% calcd) from the channels. The second weight loss between ∼450 and 750 °C corresponds to the loss of 1 mol of coordinated BDC (44.18% obsd and 43.91% calcd) molecules (Figure S2.b in the Supporting Information). In the case of compound **3**, the TGA data are not consistent with complete conversion to the oxide phase. Because **3** contains fluoride, it is assumed that some fluoride remains in the TGA residue even though the specific phase cannot be detected by XRD. For **3**, the TGA data (Figure S.2c in the Supporting Information) indicate that the release of the BDC molecules also is in two steps. The free BDC molecules are lost below 450 °C (31.03% obsd and 32.87% calcd) and the coordinated BDC above 450 °C (42.74% obsd and 43.86% calcd). In both cases, the results agree well with the formula derived from the single-crystal structure determinations and from elemental analysis.

Pyridine-Containing Phases. Synthesis and Characterization of Al(OH)BDC·py (1a) and Al(OH)BDC·0.8py (1b). Compounds **1a** and **1b** were first obtained by the reaction of the heat-treated form of a pure powder sample of **1** (380 °C, 24 h) with liquid pyridine under static conditions at 25−110 °C for 24 h. Powder XRD patterns of the products showed the presence of two related phases.

As shown in Figure 2, the initial product, Al(OH)BDC·py (**1a**), transforms to Al(OH)BDC·0.8py (**1b**) by losing pyridine in air at

ambient temperature within several hours. Compound **1a** can be recovered from **1b** by exposure to pyridine vapor (or liquid). Further investigation showed that **1a** can also be prepared by a direct synthesis: aluminum nitrate nonahydrate (1 mmol), 1,4-benzenedicarboxylic acid (1 mmol), pyridine (99%, Merck, 0.5 mL), and deionized water (10 mL) were mixed in a molar ratio of 1:2:6.2:560. The mixture was then put into a hydrothermal reaction vessel and heated at 220 °C for 3 days. The final product, a microcrystalline powder of **1a**, was collected by vacuum filtration. Elem anal. for **1a**: Al, 8.96% obsd (9.39% calcd); C, 54.00% obsd (54.35% calcd); H, 3.63% obsd (3.52% calcd); N, 4.48% obsd (4.88% calcd). Elem anal. for **1b**: Al, 9.04% obsd (9.94% calcd); C, 52.83% obsd (53.10% calcd); H, 3.61% obsd (3.35% calcd); N, 3.91% obsd (4.13% calcd).

TGA of the air-stable **1b** showed two weight losses (Figure S.3a in the Supporting Information). The first weight loss below 200 °C corresponds to the loss of 0.8 guest pyridine molecules per formula unit (23.32% measd, 23.30% calcd). The second loss corresponds to the loss of 1 mol of framework BDC molecules and occurs in the same temperature range as that for **1** (500−600 °C; 60.86% measd, 60.47% calcd). These results are also in good agreement with the elemental analysis, which gave a pyridine to framework BDC ratio of 0.83:1 for **1b**. The TGA residue was identified as Al_2O_3 by powder XRD.

The IR spectrum for **1b** (Figure S.4a in the Supporting Information) shows a drastic decrease in the intensity of the OH band, which is also slightly shifted to higher wavenumber (3704 cm^{-1}) as a result of the formation of hydrogen bonds between the intercalated pyridine molecules and the bridging OH groups. The IR spectrum for air-unstable **1a** was not recorded.

Subsequent studies showed that single crystals of **1a** could be obtained by a solvothermal single-crystal-to-single-crystal guest exchange reaction of **1** in liquid pyridine in a hydrothermal reaction vessel at 180 °C for 2 days. The powder pattern of the product was identical with that obtained by gas diffusion. A similar exchange reaction at room temperature did not lead to any noticeable reaction.

Powder XRD and Rietveld Analysis. The structures of **1a** and **1b** were determined from powder XRD data and Rietveld analysis. Initial fast scan diffraction patterns showed strong peak asymmetry especially at low angles (<23°) mainly due to the axial divergence of the X-ray beam and the effect of the low sample mass absorption coefficient (μ < 5 cm^{-1} in both compounds). The preferred orientation was also found in these preliminary scans. The data collection was improved in subsequent measurements. To reduce preferred orientation effects, powder samples were sieved onto a frosted glass square plate (30 × 30 mm). The sample axial width, length, and depth were varied to find the best conditions to minimize the peak asymmetry. On the basis of these experiments, data were collected from a sample mounted on the glass holder in a thin narrow stripe (~0.1 mm thickness, 6 mm width, and 30 mm length).

Each data set was collected in two parts with different incident beam slits and counting times to compensate for the intensity loss at high angle due to the small sample volume. Narrow slits (0.5° divergence and 1° scattering) and a 90 s counting time in steps of 0.02° were used for $5 \le 2\theta \le 25°$, while normal slits (2° divergence and 4° scattering) and a 70 s counting time in steps of 0.02° were used for $23 \le 2\theta \le 60°$. Because **1a** is unstable in air, samples were mounted on the glass holder and sealed by a polymer film (0.000 25 in.; SPEX industries). The XRD pattern has a broad feature at 23−28° from the glass plate, and this region was excluded from subsequent refinements.

Table 3. Crystallographic Data and Refinement Parameters for Compounds **1a** and **1b**

	1a	**1b**
chemical formula	$Al(OH)(C_8H_4O_4)\cdot C_5H_5N$	$Al(OH)(C_8H_4O_4)\cdot 0.8C_5H_5N$
fw	287.21	271.39
ρ_{calc} (g cm^{-3})	1.368	1.382
cryst syst	orthorhombic	monoclinic
space group	*Pnma*	*I2/a*
a (Å)	17.124(1)	6.613(1)
b (Å)	6.627(1)	11.065(1)
c (Å)	12.296(1)	17.839(2)
β (deg)		91.72(2)
V ($Å^3$), Z	1395.4(1), 4	1304.7(2), 4
T (K)	297	297
λ(Cu Kα), Kα$_2$/Kα$_1$	1.54056, 1.54439; 0.5	1.54056, 1.54439; 0.5
2θ range (deg)	5−60	5−60
no. of reflns	485	376
no. of indep atoms	21	15
no. of structural param	61	44
no. of profile param	26	26
no. of soft constraints	26	30
overall R_P	6.31	6.79
overall R_{WP}	8.64	8.67

The powder pattern of compound **1a** was found to closely resemble the simulated pattern of compound **1**. A cell indexing using TREOR gave an unambiguous orthorhombic cell with similar lattice constants. A good match was also obtained when the powder XRD pattern of **1b** was compared with the simulated pattern of $Fe(OH)(C_8H_4O_4)\cdot C_5H_5N$, which had been synthesized previously in single-crystal form. Therefore, the atomic positions from these two structural analogues were used as preliminary starting models for Rietveld analysis of compounds **1a** and **1b**, respectively.

All of the structures were refined using the *GSAS-EXPGUI* software package.[17] A polynomial function was used to adjust a set of background points manually selected until a "reasonable" curve was obtained. No refinement of the background was performed. The GSAS CW profile function #3 (a modified Thomson−Cox−Hastings pseudo-Voigt profile function) was used to determine the peak profile. Despite the use of this function, it was not possible to compensate for the peak asymmetry occurring in the low-angle part of the pattern, and this leads to higher profile reliability factors. The structure was refined by the Rietveld method with the profile parameters kept at their refined values. The atomic coordinates of models **1**)and $Fe(OH)(C_8H_4O_4)\cdot C_5H_5N$ were used as the starting values. The best results in the final stages were achieved by using soft constraints, including the Al−O, C−C, and C−O bond distances, angles, and planarity constraints. The lowest weighting factors for the different soft constraints were kept until the deformation of the chemical groups was no longer reasonable; occupancies of the channel species were fixed based on the results of TGA and elemental analysis. The overall thermal parameters for framework atoms and nonframework atoms were set as 0.025 and 0.060, respectively. No refinements on these thermal parameters were performed. In the case of **1a**, the disordered atoms in the pores were refined only at the end of the refinement because this disorder was observed previously for the model compound whose structure was solved using single-crystal data. The final agreement factors are reasonable for laboratory diffractometer data. A summary of the results of the structure refinements is given in Table 3. The corresponding final Rietveld plots are shown in Figure 3.

Synthesis and Characterization of Ga(OH)BDC·0.85py (2a). Single crystals of **2a** were obtained by a solvothermal single-crystal-to-

(17) Larson, A. C.; Von Dreele, R. B. *General Structure Analysis System (GSAS)*; Los Alamos National Laboratory: Los Alamos, NM, 2000; Report LAUR 86-748.

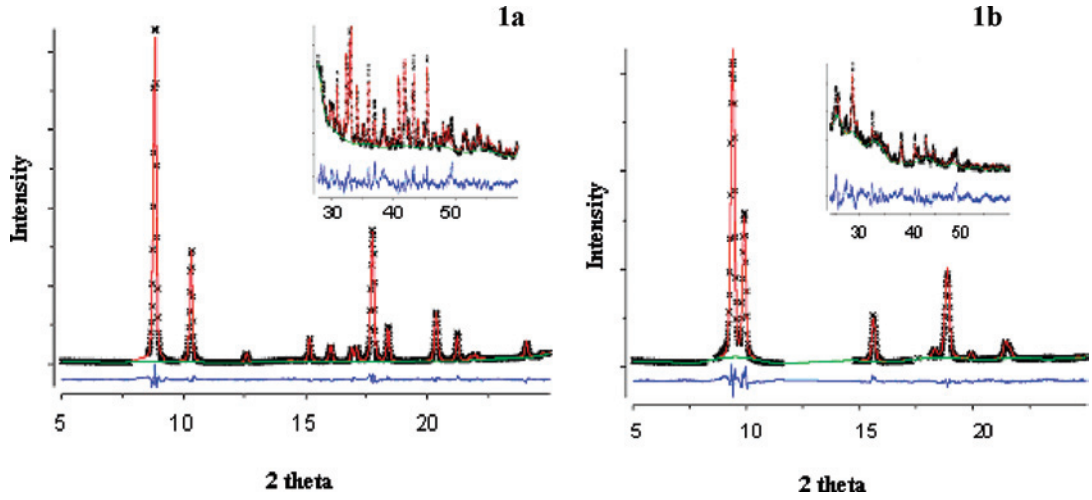

Figure 3. Observed and calculated powder XRD patterns for compounds **1a** and **1b**.

single-crystal guest exchange reaction of **2** in liquid pyridine in a hydrothermal reaction vessel heated at 160 °C for 5 days. The product, Ga(OH)BDC·0.85py (**2a**), remained crystalline and was suitable for single-crystal XRD. One single crystal of **2a** was sealed in a glass capillary containing liquid pyridine prior to the diffraction measurement. A single pyridine phase (air stable) was observed unlike in the aluminum system. Elem anal. for **2a**: Ga, 20.4% obsd (21.92% calcd); C, 45.63% obsd (46.22% calcd); H, 2.85% obsd (3.54% calcd); N, 3.58% obsd (3.74% calcd).

TGA analysis (Figure S.4b in the Supporting Information) shows that compound **2a** decomposes in two steps, losing guest pyridine below 200 °C, followed by the loss of 1 mol of framework BDC molecules at the same temperature range as that for **2** (450−550 °C; 61.91% measd, 62.60% calcd). The IR spectrum (Figure S.4b in the Supporting Information) for **2a** shows a diminution in the intensity and a shift of the OH band (to 3669 cm^{-1}) similar to those observed for **1b**.

Synthesis and Characterization of Ga(OH,F)BDC·py (3a) and Ga(OH,F)BDC·0.85py (3b). Single crystals of compounds **3a** and **3b** were obtained by a solvothermal single-crystal-to-single-crystal guest exchange reaction of Ga(OH,F)BDC·0.74H_2BDC (**3**) in liquid pyridine in a hydrothermal reaction vessel heated at 160 °C for 5 days. The crystallinity was preserved during the reaction, and one single crystal was selected and sealed in a glass capillary containing liquid pyridine prior to diffraction measurements. The results show that the sealed crystal has the composition Ga(OH,F)($C_8H_4O_4$)·C_5H_5N (**3a**) with a 1:1 ratio of gallium to pyridine. Single crystals of **3a** were exposed to air overnight, and one was mounted on a glass fiber and remeasured in air. The results confirmed that the crystals converted to Ga(OH,F)($C_8H_4O_4$)·0.85C_5H_5N (**3b**) upon exposure to air. Elem anal. for air-stable **3b**: Ga, 21.8% obsd (21.90% calcd); C, 45.54% obsd (46.17% calcd); H, 3.05% obsd (2.84% calcd); N, 3.51% obsd (3.74% calcd); F, 0.87% obsd (1.19% calcd).

As in the case of the as-synthesized compound **3**, it is assumed that the residue obtained after TGA of compound **3b** contains fluoride. The TGA data (Figure S.3c in the Supporting Information) show the loss of the pyridine molecules from within the framework at a temperature below 200 °C. If the final composition is assumed to be 80% $GaO_{1.5}$ and 20% GaF_3, then the second weight loss above 450 °C corresponds to the loss of 1 mol of framework BDC molecules (58.90% measd, 60.01% calcd). The IR spectrum for **3b** (Figure S.4c in the Supporting Information) is similar to that of **2a**.

Table 4. M−O Bond Lengths (*d*, Å) in M(OH)BDC Compounds

	d_{Al-O1}	d_{Al-O2}	d_{Al-O3}
1	1.8266(4) × 2	1.8927(3) × 2	1.8894(3) × 2
	$d_{Ga-O1(F)}$	d_{Ga-O2}	d_{Ga-O3}
2	1.896(2) × 2	1.967(2) × 2	1.970(2) × 2
2a	1.893(1) × 2	1.997(2) × 2	1.997(2) × 2
3	1.899(1) × 2	1.972(1) × 2	1.972(1) × 2
3a	1.893(4) × 2	1.968(4) × 4	
3b	1.898(4) × 2	1.989(6) × 4	

Results and Discussion

Crystal Structure Description. All eight metal (M) dicarboxylate (M = Al, Ga) compounds exhibit the same framework topology. The framework is built from M−X−M chains (X = OH, F) and bridging BDC anions, creating a three-dimensional framework with a one-dimensional diamond-shaped channel system, as was previously reported for the aluminum compound. The M^{3+} (M = Al, Ga) cation is coordinated to six oxygen atoms in octahedral geometry in the framework, with the M−O bond lengths listed in Table 4; only the results from single-crystal refinements are included.

The octahedral M−O centers are linked by sharing *trans*-hydroxyl groups (evident O−H IR band at ∼3650 cm^{-1}) or fluorine atoms, forming M−OH,F−M chains. The oxygen atoms of the BDC groups occupy the equatorial positions of the octahedra. The BDC ligands bridge the chains to form a three-dimensional framework. In all compounds, the M−(OH,F) distances are shorter than the M−O equatorial distances (see Table 4), but little variation is observed for different guest molecules in the gallium compounds.

As synthesized, the channels of compounds **1**−**3** are filled with highly disordered H_2BDC molecules (evident characteristic C=O IR band around 1710 cm^{-1}) that were modeled by partially occupied C,O positions in the structure determinations. In compound **1**, the occluded H_2BDC molecules can be removed by heating at 380−400 °C.

Pyridine Absorption by Al(OH)BDC To Give 1a and 1b. After heat treatment to remove H_2BDC molecules from the channels, Al(OH)($C_8H_4O_4$) absorbs pyridine immediately at room temperature to form **1a** and **1b**. Crystal structure studies indicate that the guest exchange reactions from

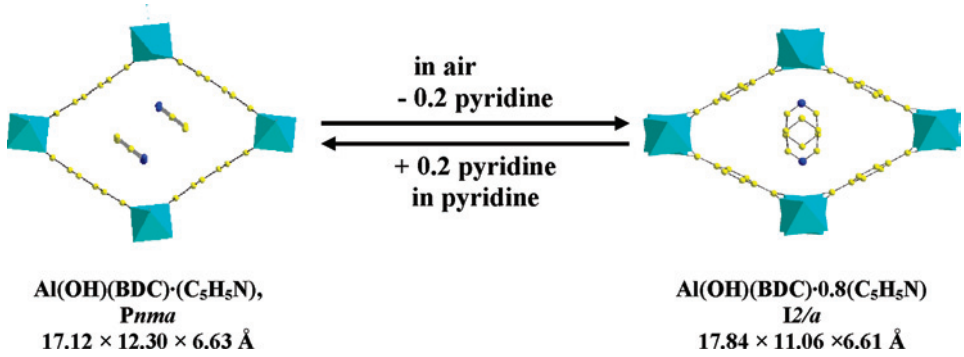

Figure 4. Schematic representation of the structural transformation that occurs upon desorption /adsorption of pyridine molecules.

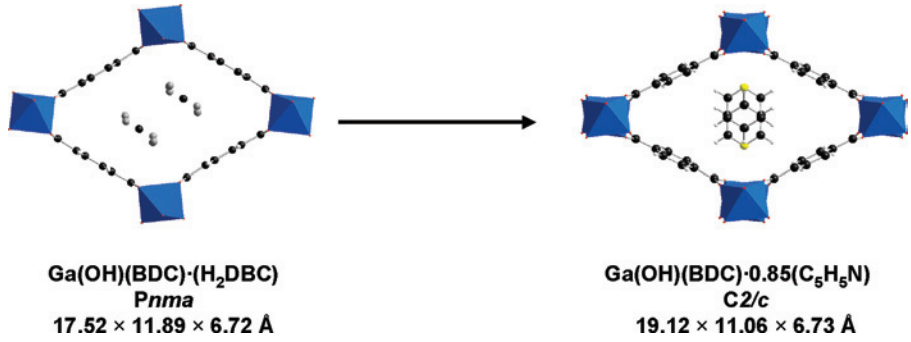

Figure 5. Schematic representation of the structural transformation upon guest exchange in the Ga(OH)BDC framework.

compound **1** occur without destruction of the framework. In compound **1a**, the pyridine molecules are ordered approximately parallel to the channel walls and are hydrogen-bonded to the bridging OH groups. Compound **1b** is isotypic with Fe(OH)BDC·0.85py,[13] where the pyridine molecules are approximately perpendicular to the channel walls and are also hydrogen-bonded to the OH groups. Upon a transition from **1a** to **1b**, the channels contract; the unit cell dimensions change from 17.124(1) × 12.296(1) Å to 17.839(2) × 11.065(1) Å and remain almost constant [from 6.627(1) to 6.613(1) Å] along the Al−OH,F−Al chain. Compounds **1a**, Al(OH)BDC·py (parallel guest orientation), and **1b**, Al(OH)BDC·0.8py (perpendicular guest orientation), are interconvertible by a relatively small change in the pyridine concentration. This transition is fully reversible and occurs on the time scale of several hours in the solid−gas reaction (Figures 2 and 4). A similar concentration-dependent change of the orientation of the pyridine guest molecules was observed in the layered compound α-$Ti(HPO_4)_2$.[18] Because the positions of the disordered guest molecules were determined from powder data, the geometry and positions of the intercalated pyridine molecules are not precisely determined. The results are consistent with those for the gallium compounds obtained from single-crystal refinements, which are discussed in more detail below.

Single-Crystal-to-Single-Crystal Guest Exchange between 2 and 2a. The single-crystal-to-single-crystal guest exchange reaction that converts compound **2** to compound **2a** also preserves the integrity of the framework. In the case of compound **2**, a higher content pyridine phase was not observed; only the pyridine-poor phase, **2a**, was recovered from the exchange. Compound **2a** is isotypic with compounds **1b** and **3b**.

The changes in the unit cell dimensions and space group that occur upon transformation from **2** to **2a** upon reaction with pyridine are shown in Figure 5. The change in the dimension along the chain axis is small. In **2a**, the pseudo-orthorhombic cell defined by the gallium atom positions has $a = 18.132$ Å, and consequently the channel area changes from 17.52 × 11.89 to 18.13 × 11.06 Å when the intercalated molecules change orientation.

The pyridine molecules are hydrogen-bonded to the hydroxyl groups that bridge the gallium atoms along the direction of the chains with a N−O1 distance of 2.744(6) Å, indicating a strong hydrogen bond. The pyridine occupancy is less than the ideal occupancy of 1 (refined as 0.78), and consequently some residual OH groups are present, as indicated by the weak band in the IR spectrum at 3669 cm^{-1}. No superstructure is observed, and so we assume that the pyridine molecules are randomly disordered among the available sites. The average planes of the pyridine molecules are parallel (more strictly, the N−O1 vector is perpendicular to the Ga−Ga vector along the chain), but disorder is apparent in the thermal ellipsoids of the pyridine carbon atoms, which are elongated along the Ga−Ga direction. The ellipsoids become much larger as one moves away from the hydrogen-bonded nitrogen atom to the furthest carbon atom, as seen in Figure 6a. The distance between pyridine rings calculated from the idealized model shown Figure 6a is too short (interplanar, 3.145 Å; between ring centers, 3.551 Å),

(18) Nunes, L. M.; Airoldi, C. *Chem. Mater.* **1999**, *11*, 2069.

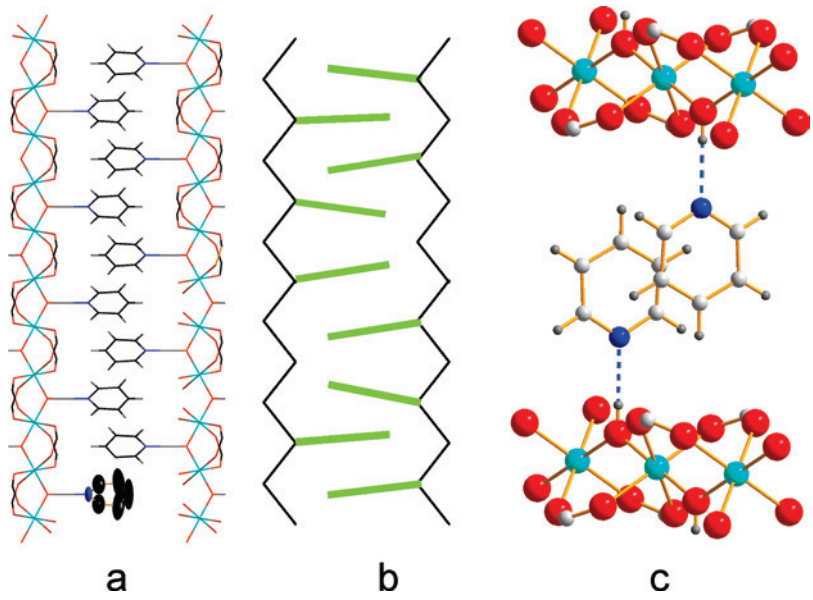

Figure 6. (a) Stick model of the idealized structure of **2a** with all OH groups hydrogen-bonded to pyridine. The thermal ellipsoids are shown for one pyridine. (b) Model for the disorder in which all of the pyridine molecules are tilted with respect to the normal to the chain axis. (c) View of the structure showing the relative orientations of adjacent pyridine molecules.

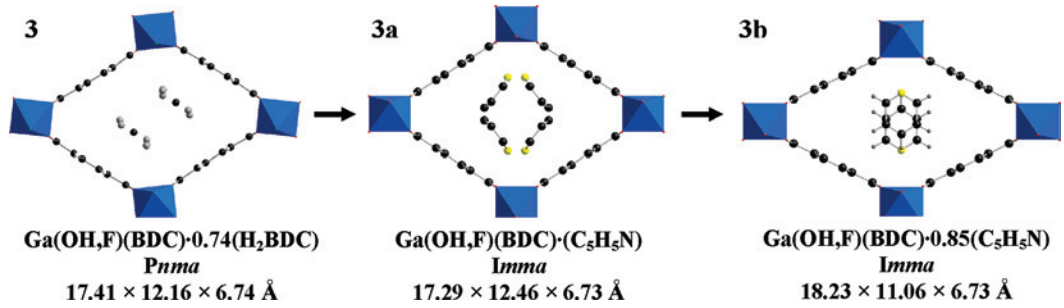

Figure 7. Structural transformations that occur when H_2BDC guest molecules in the Ga(OH,F)BDC framework are exchanged with pyridine molecules.

reflecting the fact that not all of the OH bridges are associated with a pyridine molecule. A schematic representation of the disorder with a pyridine occupancy of 0.8 is shown in Figure 6b; all of the pyridine molecules are tilted with respect to the normal to the chain axis. The relative orientations of adjacent pyridine molecules are shown in Figure 6c and suggest the possibility of some weak CH$-\pi$ interactions.

Single-Crystal-to-Single-Crystal Guest Exchange between 3 and 3a and Phase Transition to 3b. The single-crystal-to-single-crystal guest exchange reactions from compound **3** to compound **3a** also happens while preserving the integrity of the framework. Just as in the case of compound **1a**, the pyridine molecules are approximately parallel to the channel axis. However, in compound **3a**, the guest pyridine molecule is randomly disordered over two positions. **3a** is not stable in the absence of excess pyridine and, when exposed to the atmosphere, loses pyridine. The remaining pyridine molecules rearrange themselves inside the channel to be approximately perpendicular to the channel walls to give **3b**, which is isotypic with **1b**, **2a**, and Fe(OH)BDC·0.85py.

The transition from **3** to **3a** to **3b** results in a slight opening up and then closing of the channels and a change in the unit cell dimensions from 17.410(3) × 12.165(2) to 17.287(11) × 12.461(9) to 18.23(2) × 11.062(12) Å perpendicular to the channel direction; the distances parallel to the channel remain almost constant and are 6.744(1), 6.727(5), and 6.734(8) Å, respectively.

The orientation of the pyridine molecule in **3b** is similar to that observed in **1b** and in **2a**, namely, perpendicular to the chain axis direction and hydrogen-bonded to the bridging OH group [$d_{N\cdots O}$ = 2.74(2) Å]. In the presence of excess pyridine, compound **3a** is obtained containing one pyridine molecule per gallium atom. The pyridine molecules are disordered over two positions and lie parallel to the channels (see Figure 7) and are hydrogen-bonded to the bridging OH at a longer distance than that in the other orientation [$d_{N\cdots O}$ = 2.88(3) Å]. The hydrogen-bonded pyridine molecules (Figure 8a) are staggered with respect to the BDC linkers, and the predominant interactions are hydrogen bonds. One set of disordered pyridine molecules is shown in Figure 8b in the same orientation.

Conclusion

We have synthesized two new members of the M(OH)-BDC series with M = Ga in the form of single crystals with compositions Ga(OH)(BDC)·0.74H_2BDC (**2**) and Ga(OH,F)-(BDC)·0.74H_2BDC (**3**). Chemical analysis suggests that in **3** ~20% of the OH groups are replaced by fluoride ions.

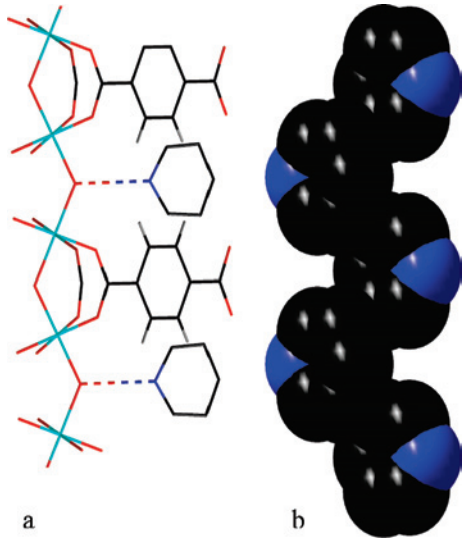

Figure 8. (a) Stick model of the idealized structure of **3a** with all OH groups hydrogen-bonded to pyridine. (b) Model showing one set of the disordered positions in the channel.

Because of the flexibility of this framework type, crystal-to-crystal transformations enable a detailed study of the intercalation of guest molecules, here pyridine.

In the case of **3**, two interconvertible guest-concentration-dependent phases with parallel (**3a**) and perpendicular (**3b**) pyridine molecule orientations are observed, which contain 1.0 and 0.8 molecules of pyridine per gallium, atom respectively. The structures are both stabilized by hydrogen bonds with the framework hydroxyl bridging groups. Similar phases (**1a** and **1b**) are formed by Al(OH)BDC, which was also synthesized in the presence of HF and probably also contains trace amounts of fluoride ions. The transformation between the two phases in both aluminum and gallium systems is completely reversible; the guest molecules can turn from one orientation to the other as the pyridine concentration is increased or decreased, a change that causes a ~7% change in the channel area. The parallel-orientation higher pyridine content phase is not observed in the absence of fluoride, most likely because of the greater relative stability of the perpendicular orientation when all of the bridging sites are available to form hydrogen bonds; partial occupancy by fluoride may lower the relative stability by making it impossible to achieve the optimum packing density (Figure 7b) in which all pyridine molecules form hydrogen bonds.

In summary, the intercalation studies presented here further demonstrate the unusual flexibility of the M^{III}(OH)BDC frameworks that can adapt their structures in response to the absorption of specific guest molecules.

Acknowledgment. We thank the R. A. Welch Foundation for support of this work.

Supporting Information Available: X-ray crystallographic data, in CIF format, for the structure determinations of **1**, **2**, **3**, **2a**, **3a**, and **3b** and TGA data and IR spectra for **1**, **2**, **3**, **1b**, **2a**, and **3b** in PDF format. This material is available free of charge via the Internet at http://pubs.acs.org.

IC800008F